Multiscale mathematical biology of cell-extracellular matrix interactions during morphogenesis

Rens, E.G.

4

From Focal Adhesion Dynamics to Cell Shape Changes and Durotaxis: a multiscale cell-based model

This chapter is based on:

Rens EG and Merks RMH (2018) *From Focal Adhesion Dynamics to Cell Shape Changes and Durotaxis: a multiscale cell-based model* (in preparation).

Abstract

Cells adapt their behavior in response to physical properties of the matrix, such as matrix stiffness. Cells are able to sense the mechanical properties of the matrix through transmembrane integrin molecules, which assemble into large multimolecular complexes called focal adhesions. Focal adhesions grow and assemble in response to force application. Here we show with a multiscale cell based computational model that force based growth of focal adhesions suffices to explain the response of cells to substrate stiffness. We base our model on the fact that individual integrins within focal adhesions, such as $\alpha_5\beta_1$, have been shown to behave as catch-bonds; special bonds whose lifetime is maximal under positive force. In our model, cells apply a contractile force on integrin clusters. How fast this force builds up, depends on the stiffness of the substrate. The integrin clusters then grow according to catch-bond dynamics. These integrin clusters affect the probability of a cell detaching from the substrate. The model can accurately predict cell area as a function of substrate stiffness. The model can also reproduce cell elongation when we added another force based molecular mechanism of focal adhesions; where matrix stresses induces adhesion strengthening. The model suggests that the stiffness regime on which cells elongate is regulated by the velocity of its myosin motors. Furthermore, our model reproduces durotaxis, suggesting that is regulated by a bias in integrin clustering due to the catch-bond behavior of integrins.

4.1 Introduction

Embryonic development, structural homeostasis and developmental diseases are driven by biochemical signals and biomechanical forces. By interacting with the extracellular matrix (ECM), a network of fibers and proteins that surrounds tissues, cells can migrate and communicate with other cells, which contributes to tissue development. Mechanical interactions between cells and the ECM are crucial for the formation and function of tissues. By sensing and responding to physical forces in the ECM, tissues can adapt accordingly.

In particular, many mammalian cells change their shape and migrate in response to matrix stiffness. On soft matrices, cells are small and rounded, while on stiffer matrices cells are elongated. On matrices of glass like rigidity, cells can spread out like pancakes. This behavior has been observed for many cell types (endothelial cells: [199], fibroblasts: [129, 200], smooth muscle cells: [201], osteogenic cells: [202]), although the range of stiffness on which the cell becomes elongated varies between cell types [203, 204]. Another generic cell behavior is durotaxis, cell migration upwards a stiffness gradient [127, 205, 206]. However, it is still poorly understood what molecular mechanism regulates cell response to matrix stiffness [207].

Cells are able to sense matrix stiffness through focal adhesions, which are multimolecular complexes consisting of integrin molecules and structural proteins [208]. Integrins are receptors for ECM proteins and mediate cell-ECM binding and force transmission. Structural proteins, such as vinculin and talin, bind integrin to actin

stress fibers in the cytoskeleton. On compliant matrices, adhesions dynamically assemble and disassemble, while on more stiff matrices, focal adhesions stabilize [129]. Such mechanosensitivity of focal adhesion assembly is regulated by molecular components, like talin and p130Cas, that change conformation in response to mechanical force [207, 208], which allows focal adhesions to assemble or disassemble in response to forces. For instance, stretching the structural protein talin reveales vinculin binding sites, allowing additional vinculin to bind to focal adhesions [209] and stabilize the adhesion [210]. Also, integrins such as $\alpha_5\beta_1$, behave as "catch-bonds" [211], bonds of which the lifetime increases under force [212]. Because focal adhesions regulate cell spreading, orientation and migration [213–218], the mechanosensitive growth of focal adhesions is the key to our understanding of how cells respond to matrix stiffness.

Previous mathematical models proposed that cell spreading on compliant matrices is due to dynamic reciprocity: cells apply a force to the matrix and respond to the reaction of the substrate by changing cellular activities. On stiff matrices, cells experience more stress, as the matrix does not deform. If this stress positively feeds back on cellular traction forces, a cell can polarize because an initial asymmetric cell shape is reinforced by this feedback mechanism [48]. Similarly, it was proposed that cells elongate because of a positive feedback loop between contraction and strain stiffening of the matrix [183]. A feedback between stress induced recruitment of motor proteins and increased traction forces has been proposed to regulate cell spreading [219].

Other mathematical models predicted cell spreading by integrating a focal adhesion model into a cell-based model [220–222]. In these models, it was assumed that stress induces the recruitment of adhesive molecules [49, 50]. It was proposed that as substrate stiffness increases, stress fibers become more tensed and thus apply larger forces which stabilizes focal adhesions and allows a cell to spread [220, 221]. These models included many variables, including cytoskeleton/actin fiber dynamics, adhesion dynamics and their interactions. This made it difficult to dissect how exactly cell shape changes are regulated. A model including focal adhesions but no stress fiber dynamics could predict the localization of focal adhesions in a cell but could not explain increased cell area on stiffer matrices [222]. So, it is still not clear what the minimal condition is for cell spreading in response to matrix stiffness.

A range of mathematical models have also been used to explain durotaxis. For instance, it was proposed that the mechanosensitivity of stress fibers regulates durotaxis. It was suggested that a stress fiber becomes more tensed and thus stabilizes if it attaches to a stiff substrate, which results in movement up the stiffness gradient [223]. Another model proposed that a stress fiber durotacts because tensing of a stress fiber resulted in faster sliding of adhesions on the softer side of the matrix [224]. It has also been suggested that cell polarization drives durotaxis. It was proposed that cells durotact by polarizing more on stiffer substrates [225] or by polarizing towards stiffer substrates [226]. Furthermore, it was proposed that durotaxis is driven by a stiffness mediated traction force [227], bias in velocity [228], viscous force and cell stiffening [229], motor protein recruitment [219], cell-matrix adhesion strength [230] or persis-

tence time [231]. Many of the proposed mechanisms for durotaxis [225, 227, 228, 230] are based on the fact that focal adhesions stabilize on stiff matrices, but it is still poorly understood how the mechanosensitive growth of focal adhesions can drive durotaxis.

By integrating a focal adhesion model in a cell-substrate model, we show that dynamic reciprocity through focal adhesion dynamics are sufficient to explain three important cell generic phenonema 1) cell area increases with matrix stiffness; 2) cell elongation depends on matrix stiffness; 3) durotaxis. We model focal adhesions as clusters of integrin-ligand bonds and assume that the unbinding of integrin bonds decreases with force [232]. The cells pull on these clusters and the rate of force build-up depends on the matrix stiffness [97]. In our cell based model, we assume that cell-matrix adhesion strength increases with integrin cluster size. This model explains cell spreading as a function of substrate stiffness. We also include an adhesion strength reinforcement due to matrix stresses. This matrix stress feedback allows cells to elongate on matrices of intermediate stiffness. We show that the range of stiffness on which cells elongates depends on the velocity of myosin motor proteins. Finally, our model suggests that durotaxis speed increases with the slope of the stiffness gradient.

4.2 Results

Using a multiscale computational model, we propose that focal adhesion dynamics can explain cell spreading, cell elongation and durotaxis in response to substrate stiffness. Figure 4.1 gives an overview of the model, showing the flow and feedback between the cell, its focal adhesions and the elastic substrate it adheres to. In a first version of our model (M1), we only follow the loop with arrows 1 and 2 in the flowchart, thus excluding a feedback with matrix stress. We start out with model M1, to study how this minimal model, which describes focal adhesions as clusters of catch bonds, translates to cell spreading.

Model M1 proceeds as follows. A cell is described as a collection of discrete lattice sites in a cellular Potts model (CPM), see Figure 4.1A. The cell applies a contractile force upon focal adhesions that adhere to the matrix. We use the shape of the cell to calculate the contractile force based on a First Moment of Area (FMA) model [132], see Figure 4.1B. Because focal adhesions adhere to the substrate, how fast a cell can build up this force, depends on the substrate stiffness. We adopt a model of Schwarz *et al.* [97] to describe the build up of force in time due to myosin motor activity: $F(t) = F_s(1 - \exp(-t \cdot \frac{v_0 K}{F_s}))$, with v_0 the free velocity of the motor proteins and K the substrate stiffness. So, in model M1, matrix stiffness only affects the rate of force build-up. The more compliant the substrate is, the longer it takes for a cell to build up this force. In part B of the model, we let the forces build up for t_{FA} seconds. At the same time, part C of the model is executed. At each site of the CPM, a focal adhesions is defined (see Figure 4.1C) as a cluster of bound integrin bonds. We assume that the growth of each integrin cluster is a function of the force it experiences, according to the catch-slip bond behavior described as an ODE proposed by Novikova and Storm [232].

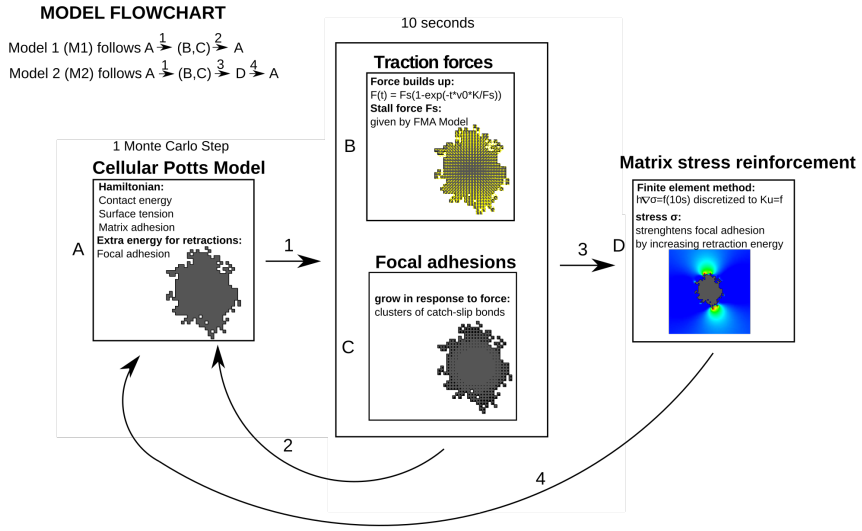

Figure 4.1: Flowchart of the multiscale CPM. (A) CPM calculates cell shapes in response to focal adhesions and substrate stresses; (B) calculation of cellular traction forces based on cell shape and force build-up dynamics; (C) focal adhesion grow according to dynamics of catch-slip bond clusters; and (D) calculation of substrate stresses due to cellular traction forces.

Simultaneously with the force build-up, we let the integrin clusters grow. After these t_{FA} seconds, we perform one timestep in the CPM. Cells in the CPM change shape by iteratively making extensions and retractions, modeling the formation and break down of adhesions with the substrate. We assume that retractions from the substrate are less likely at sites with larger integrin clusters. After one timestep of the CPM, we again let the forces build up and the integrin clusters grow for t_{FA}, and so forth.

4.2.1 Integrin catch-bond dynamics suffices to predict cell area as a function of substrate stiffness

In this section, we show with model M1, that catch-bond dynamics of integrin bonds suffices to explain cell spreading on elastic substrates. Figure 4.2A shows the response of cells on substrate of 500 μm by 500 μm with a Young's modulus of 1 kPa, 5 kPa, 10 kPa, 20 kPa, 50 kPa, 100 kPa and 10^8 kPa after 2000 MCS (≈ 5.5 h). On the most soft substrate, focal adhesions do not grow and the cell does not spread. On a slightly stiffer substrate of 5 kPa, focal adhesions have grown and the cell has significantly increased in size. Increasing the substrate further also increases the cell area, although from 50 kPa the cell does not seem to change in size. On stiffer substrates, there are more larger focal adhesions visible and they seem to accumulate more around the cell membrane, as shown in the two insets in Figure 4.2A.

Figure 4.2B plots the cell area as a function of substrate stiffness. Cell area increases from around 2500 μm^2 on the softest substrate and plateaus at around 6500 μm^2 at a stiffness of 50 kPa. Thus, the cell area has increased more than 2.5 fold on the stiffest substrate compared to the softest substrates. This factor is consistent with experimental observations [199, 233, 234]. We also investigated if the model could quantitatively predict spreading dynamics. Figure 4.2C plots the cell area as a function of time. The cells quickly increase in size and and reach their final size after 30 to 60 minutes. Experimental curves of cell area versus time follow a similar trend [124, 203].

We also investigated the distribution of the integrin cluster sizes. Figure 4.2D plots the distribution of the cluster sizes and the median cluster size (average cluster size is roughly the same). The median cluster size and variance are unaffected by substrate stiffness, in contrast with experimental observations [235]. We performed a more detailed analysis of the distribution of integrin clusters and describe two observations. 1) On stiffer substrates, there are more larger clusters. For instance, the percentage of adhesions with $N > 10000$ is 20% on 50000 kPa, 15% on 10 kPa and 10% on 5 kPa. 2) On stiffer substrates, large focal adhesions are found at the cell boundary (Figure 4.2A for 50 kPa and Supplementary Figure 4.6). On soft substrates, large focal adhesions are found further away from the cell center, where forces had time to build up because in the bulk of the cell no retractions take place (Figure 4.2A for 5 kPa and Supplementary Figure 4.6).

All in all, the results presented in this section suggest that the catch-slip bond dynamics of single integrins within focal adhesions suffice to predict cell area and spreading dynamics from substrates stiffness. Our model explains that cells spread due to intertwined dynamics of force build-up, focal adhesion growth and cell-matrix adhesion. On soft substrates, forces build up slowly, so there is not enough time for a focal adhesion to grow to strongly adhere the cell to the matrix. So, the cell will continuously make extensions and retractions. In contrast, on stiff substrates, forces build up fast and focal adhesions are able to grow and extensions have a long lifetime, allowing the cell to spread.

4.2.2 Adhesion strengthening due to matrix stress induces cell elongation

After having captured, at a quantitative level, the rate of spreading as a function of substrate stiffness, we now set out to explain the ability of mammalian cells to elongate on stiff enough substrates. Because the first version of the model (M1) could not yet explain cell elongation, we aimed to find an additional focal adhesion mechanism that can explain cell elongation.

Since cell traction forces are transferred to the matrix through the integrins, stresses develop in the matrix. Such stresses have been observed to affect focal adhesion assembly [217]. We therefore hypothesized that such a feedback may explain cell shape changes. We extended our model to Model M2, that includes a finite element model to calculate the matrix stress (Figure 4.1D) as a result of the cell traction forces. So,

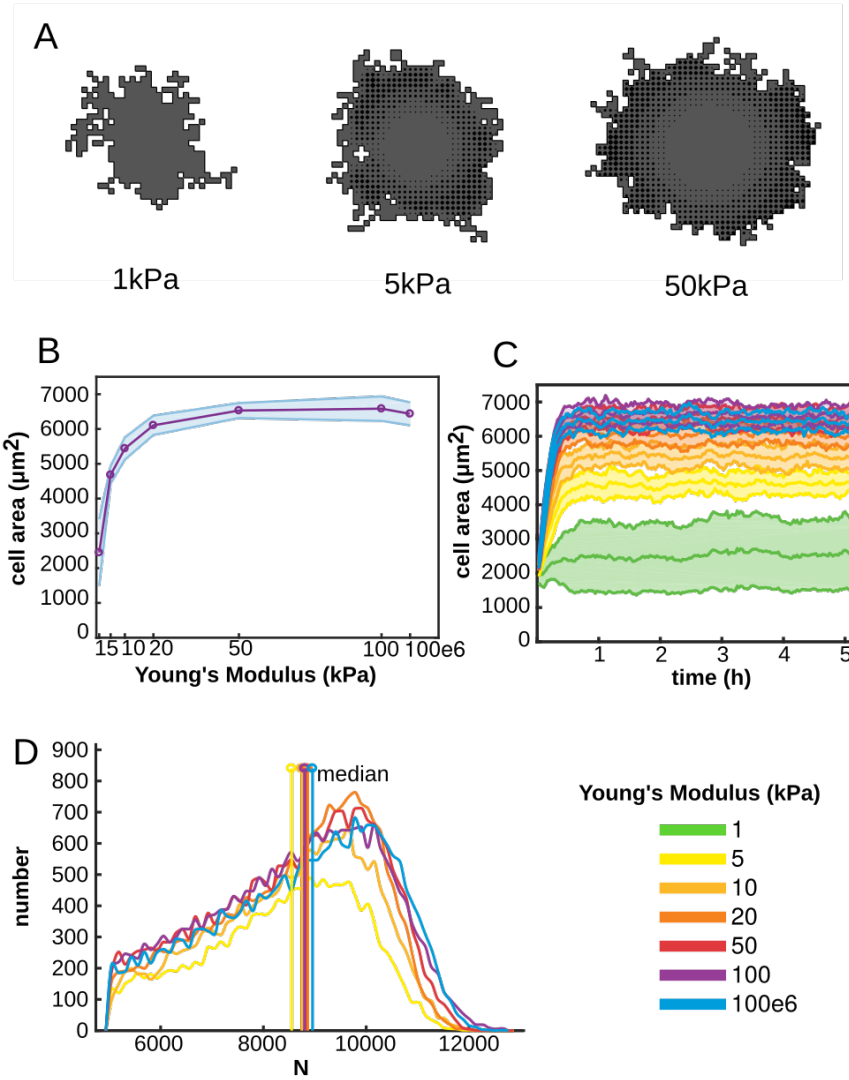

Figure 4.2: Cell area increases with increasing substrate stiffness. Model M1 was used. (A) Example configurations of cells at 2000 MCS on substrates of 1,50 and 50 kPa; (B) Cell area as a function of substrate stiffness, shaded regions: standard deviations of 25 simulations; (C) Timeseries of cell area, shaded regions: standard deviations of 25 simulations; and (D) distribution of N, the number of integrin bonds per cluster, all clusters at 2000 MCS from 25 simulations were pooled. We indicate the median. Color coding (C and D): See legend next to (D).

model M2 follows arrows 1, 3 and 4 in Figure 4.1D. We assume that matrix stresses reinforces cell-matrix adhesions. We model adhesion strengthening by reducing the probability of retractions from the matrix due to matrix stress, *i.e.* we multiply the energy it takes for a cell to make a retraction with $1 + p\frac{g(\underline{\underline{\sigma}}(\vec{x}))}{\sigma_h + g(\underline{\underline{\sigma}}(\vec{x}))}$. Here, parameter p regulates the strengthening and σ_h its saturation and $g(\underline{\underline{\sigma}}(\vec{x}))$ denotes the hydrostatic stress on the lattice site of retraction. Such a strengthening due to matrix stress can have various molecular origins. We hypothesize that this strengthening is due to stretching of the structural protein talin exposes binding sites for vinculin, which binds to the cytoskeleton and thus strengthens the actin-integrin linkage [209, 210].

Figure 4.3A shows representative configurations of cells after running model M2. Similar to model M1, on the most soft substrate (1 kPa), the cell stays small and round. From around 10 kPa/20 kPa, the cells start to slightly elongate. On stiffer matrices, 50 kPa and 100 kPa, cells are very much polarized in shape and large focal adhesions have grown at the tips of the cell. On the very rigid substrate, the cell is more circular again. To quantify cell elongation, we measured the eccentricity of cells as $\sqrt{(1 - \frac{b^2}{a^2})}$ with a and b the lengths of the cell's major and minor semi-axes, calculated as the eigenvalues of the inertia tensor. Figure 4.3B shows that the eccentricity of cells has a biphasic dependence on substrate stiffness. We also again quantified the distribution of the integrin cluster size again. Figure 4.3C shows the distribution of the cluster sizes for the different elastic substrates. The median cluster size does not vary much between substrate stiffness. The shape of the distributions, however, is much more flat and with higher variance on the substrates where cells have elongated. This is because an elongated shape results in large traction force at the tip of the cells, such that focal adhesions grow larger in size there, while at the sides of the cell, the forces are much smaller and focal adhesion stay small there.

The model explains the process of cell elongation as follows. On sufficiently stiff matrices, the cell initially starts to spread. The cell continuously makes random protrusions, allowing the cell shape to become slightly anisotropic. Around these cell protrusions, matrix stresses develop, which strengthens cell-matrix adhesion in this region. So, the cell can continue to build up forces, allowing the focal adhesion to grow larger. In contrast, at site of lower matrix stress, focal adhesions are more likely to disassemble. At protruding sites, cell traction forces increase due to an increased distance from the cell centroid. This results in a breaking of symmetry and the cell starts to elongate due to a positive feedback loop of force build-up, focal adhesion growth and matrix stress induced adhesion strengthening. On soft matrices, matrix stresses are not high enough to initiate a symmetry breaking. On the most rigid surface, matrix stresses are too high, allowing adhesions to strengthen equally well such that no symmetry breaking can occur. So, cell elongation is only possible on substrates with an optimal rigidity. Similar dynamics of cell spreading followed by a symmetry breaking has also been observed experimentally [215]. Note that the spindle-like shape that cells obtain in our model is similar to observed *in vitro* [128].

Some parameters, such as p and σ_h were chosen arbitrarily. So, we tested the sensi-

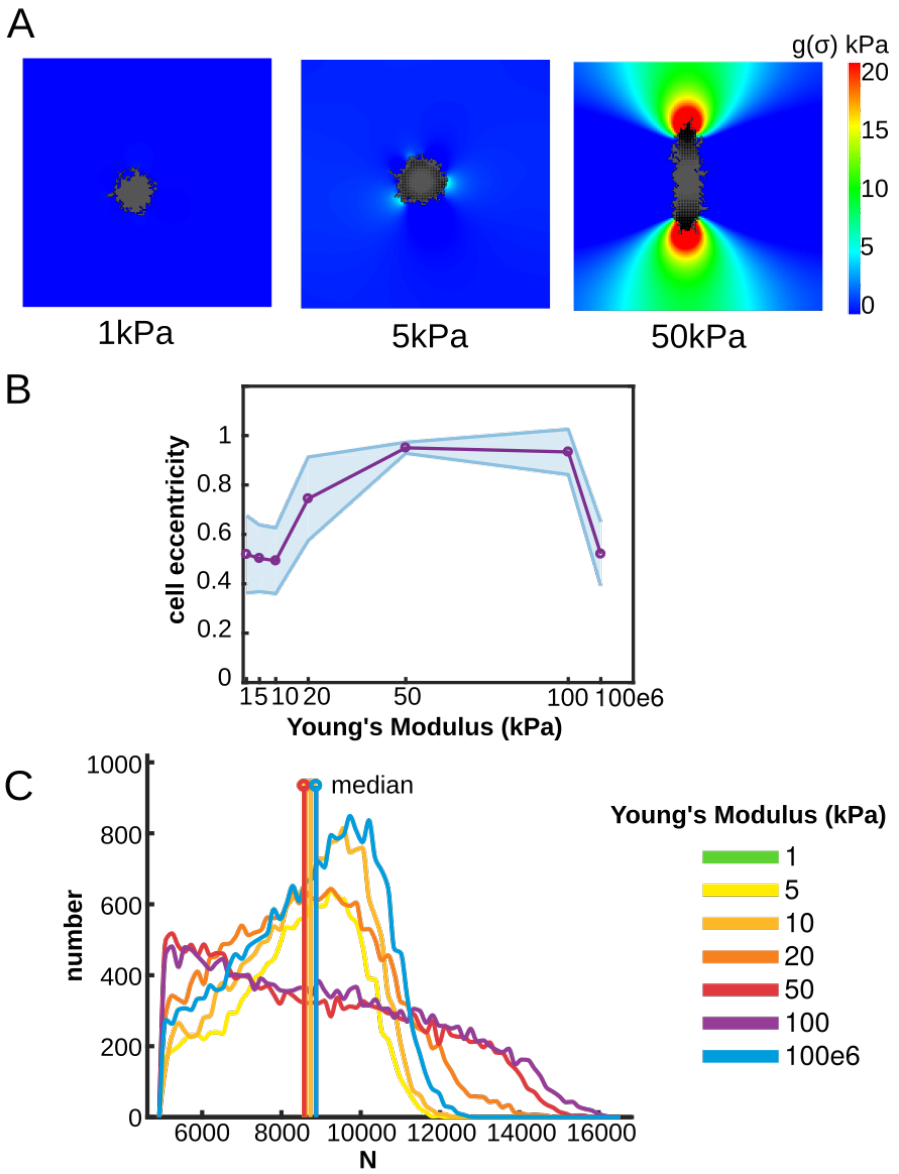

Figure 4.3: Cells elongate on substrates of intermediate stiffness. Model M2 was used. (A) Example configurations of cells at 2000 MCS on substrates of 1,50 and 50 kPa. Colors: hydrostatic stress; (B) Cell eccentricity as a function of substrate stiffness, shaded regions: standard deviations of 25 simulations; (C) distribution of N, the number of integrin bonds per cluster, all adhesion at 2000 MCS from 25 simulations were pooled. We indicate the median. Color coding (C): See legend next to (C).

tivity of our model M2 to these parameters. Increasing p which regulates the extend of adhesion strengthening by matrix stress, enables cells to start elongating on softer matrices and also induces cell elongation on the most rigid surface (Supplementary Figure 4.7). Variations in σ_h, which regulates the saturation of stretch exposed binding sites for vinculin does not greatly affect model behavior (Supplementary Figure 4.8). Other parameters might be cell type specific, such as the lifetime of protrusions t_{FA} (Supplementary Figure 4.9), extent of random motility T (Supplementary Figure 4.10) and the magnitude of traction forces μ (Supplementary Figure 4.11). The qualitative behavior is conserved for variations of these parameters, but all parameters affect the range of substrate stiffness on which the cell can elongate.

Symmetry breaking due to matrix stress can also occur by a matrix stress mediated increase in traction force. If, instead of adhesion strengthening, we assume in our model that the stall force increases as a function of matrix stress, *i.e.* $\vec{F}_s = \vec{F}_s \cdot \left(1 + p \frac{g(\sigma(\vec{x}))}{\sigma_h + g(\sigma(\vec{x}))}\right)$, we obtain similar results as in Figure 4.3 (see Supplementary Figure 4.12). Such a mechanism can have various molecular origins. For instance, addition of vinculin through talin stretching can induce increased traction forces [236]. Stretching also induces α-smooth muscle actin recruitment to stress fibers [237], and myosin motor binding [238].

In conclusion, our model suggests that by applying a force on the matrix, cells develop an anistropic matrix stress field that can induce a symmetry breaking of the cell by reinforcing adhesion sites. This allows a cell to elongate on substrates of intermediate stiffness. Such a matrix stress reinforcement can be from various molecular origins, such as a matrix stress induced adhesion strengthening or increased traction forces.

4.2.3 Motor protein velocity changes stiffness regime on which cells elongate

The regime of substrate stiffness on which cells spread and elongate varies per cell type. For instance, neutrophils do not respond to changes of substrate stiffness in the range of substrate stiffness where both fibroblasts and endothelial change in area and shape [203]. To try and understand why this is the case, we can vary cell related parameters in our model. One cell specific parameter is the velocity of the myosin motors. Many cells express non-muscle myosin II, which exists in isoforms A,B and C [239]. Other cell types also expresses myosin isoforms such as skeletal, cardiac and smooth muscle myosin [239]. Different cell types may have different expression profiles of myosin isoforms [240] and since the velocity of myosin motors varies among isoforms [241, 242], this may impact the response of cells to matrix stiffness. Using our model, we study how myosin motor velocity, v_0, can impact cell shape. We study a range from 10 nm/s (order of non-muscle myosin II B [241]) to 1000 nm/s (can be achieved by muscle myosin [243]).

Figure 4.4A and B shows the cell configurations for a slow (10 nm/s) and fast motor velocity (1000 nm/s), compared to the default value of 100 nm/s as shown in Figure 4.3A, respectively. This shows that cells with slow motors do not spread signifi-

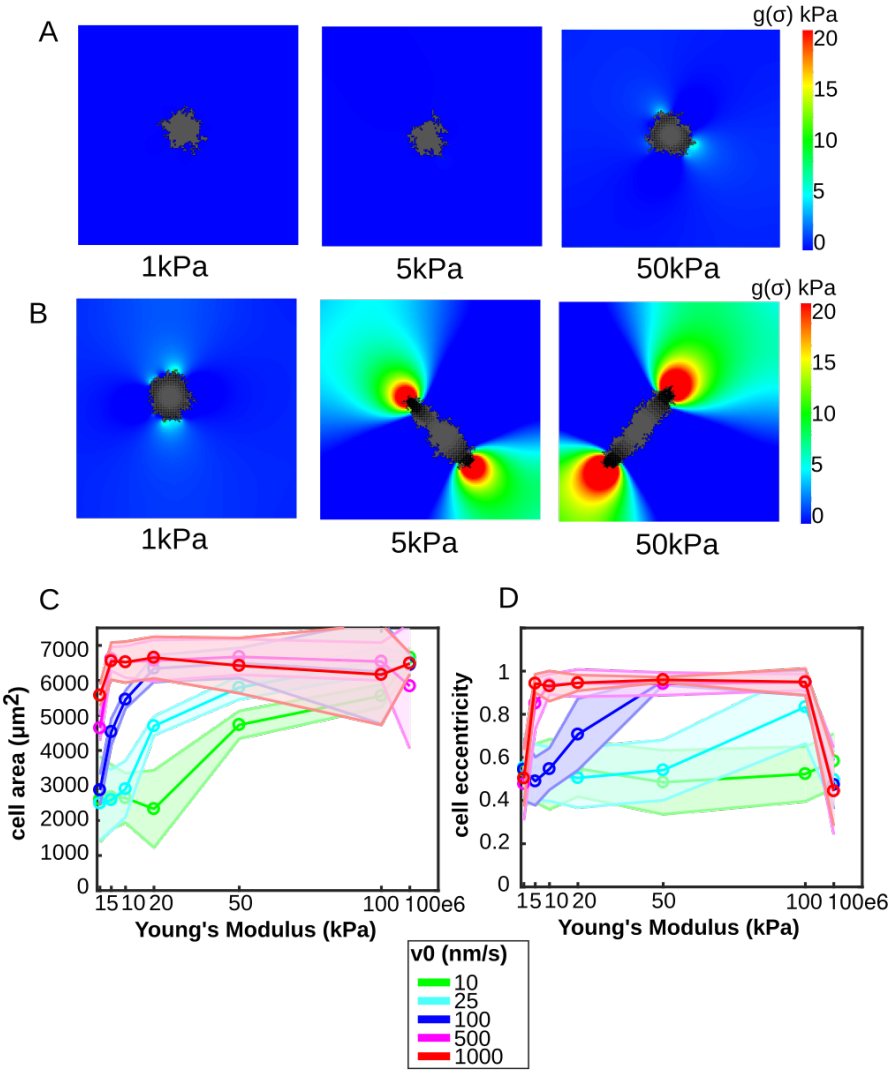

Figure 4.4: Range of stiffness on which cells elongate depends on myosin motor velocity. Model M2 was used. (A) Example configurations of cells at 2000 MCS on substrates of 1,50 and 50 kPa with motor velocity 10 nm/s; (B) Example configurations of cells at 2000 MCS on substrates of 1,50 and 50 kPa with motor velocity 1000 nm/s. Colors (A-B): hydrostatic stress; (C) Mean cell area as a function of motor velocity, error bars: standard deviations of 25 simulations; (D) Mean cell eccentricity as a function of motor velocity, error bars: standard deviations of 25 simulations.

cantly and do not elongate, even on stiffer substrates. In contrast, cells with fast motors already spread more and elongate on softer matrices. We quantified this further by running 25 simulations for each combination of substrate stiffness and motor velocity. Figure 4.4B and Figure 4.4C plot the cell area and eccentricity, respectively, as a function of motor protein velocity. With the fastest velocity tested here (1000 nm/s), cell area saturates already at 5 kPa and cells elongate on a larger stiffness regime (5 kPa - 100 kPa). With the slowest motor velocity (10 nm/s), cells do not elongate at all, while they still spread well on stiff matrices. This is explained as follows. Decreasing v_0 is very similar to decreasing the stiffness of the substrate, because they both contribute to the rate of force build-up in the same way, given by $\frac{|\vec{F}_s|}{v_0 K}$. So, in terms of cell area, cells with slower motor proteins would obtain a larger spreading area at stiffer matrices. However, they are not able to elongate because forces are not built up fast enough to generate high enough matrix stress that induces the adhesion strengthening.

So, in summary, we predict that cells with faster motor proteins start spreading/elongating at softer substrates, while cells with slower motor proteins need a stiffer substrate to instigate a response.

4.2.4 Durotaxis explained by a bias in integrin clustering

On substrates with a stiffness gradient, cells move up the stiffness gradient, a phenomena called durotaxis. Cells may durotact by sending out protrusions which better stick to stiff substrates because focal adhesions grow on stiff substrates [127, 244]. Here, we investigate if force induced focal adhesion growth is sufficient to reproduce durotaxis. We simulated durotaxis by placing an initial circular cell with its center at x=y=250 μm on a grid of 1250 μm by 500 μm for 10000 MCS ($\approx 28h$). In the x-direction, we let the stiffness increase from 1 kPa to 26 kPa, so with a slope of 20 Pa/μm. Figure 4.5A plots ten different trajectories of the cell, showing that most cells have moved significantly in the x-direction, up the stiffness gradient. Cells, on average, move in the x-direction with a constant speed of around 4.3 μm/h, measured as the slope of the x-coordinate of the cell from 25 simulations. Vincent *et al.* [206] found speeds of 6.2 μm/h with gradient slope 10 Pa/μm *in vitro* for mesenchymal stem cells. In our model, how far cells can move up the gradient, depends on the flexibility and motility of the cell. We varied λ, the Lagrangian multiplier of the area constraint, controlling cell flexibility, and the cellular temperature T, and found that both affect cell speed (Table 4.2).

In the CPM, cell movement is a result of subsequent protrusions and retractions. In stiffer areas the focal adhesions grow larger, so that retraction are more likely to be made at more flexible parts of the matrix. As a result, the cell moves up the stiffness gradient. So, naturally, one would expect that durotaxis depends on the slope of the stiffness gradient. Figure 4.5B shows the speed of the cell as a function of the slope of the stiffness gradient. Indeed, simulated cells move faster up the gradient if the slope is steeper, as observed in experimental conditions [205, 206]. This is because the difference in focal adhesion growth between the front and the back of the cell is larger with a higher slope, causing a larger bias. We suspect that the durotaxis speed saturates

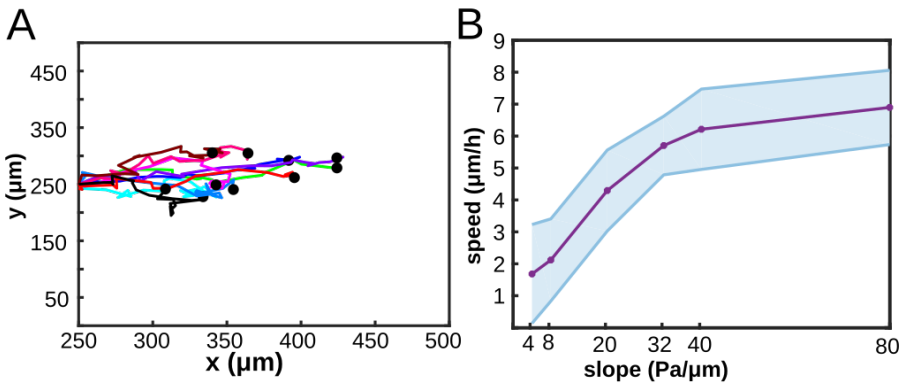

Figure 4.5: Durotaxis as a result of integrin catch-bond dynamics. (A) Ten trajectories of durotacting cells on a matrix with slope 20 kPa/ µ m; (B) Cell speed as a function of the slope of the stiffness gradient.

at steep slopes, because the growth rate of focal adhesions is limited.

In conclusion, durotaxis is an emergent behavior in our model, cells exhibit durotaxis as a result of a biased growth of focal adhesions. A cell can build up forces faster on stiffer matrices, allowing focal adhesions to grow larger here. So, the cell better attaches at the stiffer part and will retract at the softer side. As a result, the cell moves up the stiffness gradient.

4.3 Discussion

We have presented a multiscale computational model to show that force induced focal adhesion dynamics can explain 1) cell area increasing with substrate stiffness (Figure 4.2A-B), 2) cell elongation on substrates of intermediate stiffness (Figure 4.3A-B) and 3) durotaxis (Figure 4.5A). The model described cells spreading on an elastic substrate via focal adhesions, which are modelled as integrin clusters. Cells applied traction forces on integrin clusters, which grow according to catch-slip bond dynamics as proposed by Novikova and Storm [232]. How fast a cell in our model can build up this force depended on the stiffness of the matrix, based on a model by Schwarz et al. [97]. On soft matrices, forces build up slowly such that integrin clusters do not have enough time to grow, while on stiff matrices forces build up fast such that integrin clusters can grow in size. Because we assumed that larger focal adhesions detach less likely from the substrate than smaller ones, cell spreading area increased on stiffer substrates (Figure 4.2B). If we included a feedback between matrix stresses and cell-matrix adhesion, simulated cells were able to elongate. Based on experimental observations [217], we assumed that matrix stress stabilizes focal adhesions. We modeled this by reducing the likelihood of cell-matrix deadhesion. This allowed cells to elongate on matrices of

intermediate stiffness (Figure 4.3A-B). The model suggests that the range of substrate stiffness on which cells elongate depends on the velocity of the myosin molecular motors, which determine the rate of force build-up. Cells with higher motor protein velocity started to elongate on softer matrices (Figure 4.4). Finally, our model explains durotaxis as a bias in focal adhesion growth on stiffer matrices. Because extensions are more likely to stick at these regions and retractions are more likely to be made on the softer side, cells obtain a bias in cell motility up the stiffness gradient (Figure 4.5A). Our model predicted that cell velocity increases with the slope of the stiffness gradient (Figure 4.5B), which compares well with experimental data [205, 206]. The spreading dynamics in our model also qualitatively compare well with *in vitro* dynamics: the spreading dynamics in Figure 4.2C are similar to spreading area curves found *in vitro* [124, 203] and the dynamics of cell elongation (Movie S1) resemble *in vitro* observations [215].

We hypothesized that the stabilization of focal adhesions by matrix stress is due to stretching of talin. Stretching of talin exposes vinculin binding sites [209] and vinculin in turn binds the focal adhesion to the cytoskeleton, which strengthens cell-matrix adhesion [210]. Our model suggests that this might regulate cell elongation. In agreement with this observation, vinculin regulates cell elongation on glass substrates [213]. We could attempt to further unravel how vinculin drives cell elongation by studying vinculin depleted cells on substrates of different stiffness, or by adapting talin in such a way that vinculin cannot bind as a result of talin stretching.

Interestingly, our model suggests that cells can also elongate if matrix stress induces an increase in cell traction forces (Supplementary Figure 4.12). This mechanism can be justified by two experimental observations; 1) vinculin increases cell traction forces [236] and 2) stressing focal adhesions induces α-smooth muscle actin recruitment to stress fibers that in turn increases traction forces [237]. Experimental testing can be done to elucidate which mechanism might be required for cell elongation, since our model does not differentiate between these two and vinculin adhesion strengthening.

Our model also predicts that cells elongate on different ranges of substrate stiffness, due to different velocities of their myosin motors (Figure 4.4). This could explain why different cell types elongate on different stiffness regimes [203, 204], as they might express different isoforms of myosin motors. Many studies of different types of cells on compliant substrates have been performed, but often either the range of substrate stiffness tested differs or the type of matrix (*i.e.* type of ligand, ligand density, or gel type) is different. Therefore, spreading of different cell types cannot be compared one to one. Model validation would benefit from more systematic *in vitro* experiments of different cell types on compliant matrices. To then confirm this model prediction, it could be measured which isoform of myosin the cells express. There are some experiments that seem to support our model prediction. For instance, cell elongation is promoted in Dlc1 deficient ovarian tumour [245]. Dlc1 leads to increases of phosphorylation level of non-muscle IIA mysosin [245], which suggests that an increase in motor protein velocity indeed enables cells to elongate more. Furthermore, cells treated with blebbistatin on

stiff matrices obtain phenotype as if they are on a soft matrix [246], while upregulating myosin gives opposite results. In this paper by Jiang et al. [246] it was suggested that the actomyosin pulling speed produce has a similar effect on integrin stem cell lineage specification (which is highly associated with cell shape [247]) as the effective spring constant of the substrate.

The strength of our model is that we can associate response of cells to matrix stiffness with mechanisms at the level of adhesions. In our model, we differentiate between integrin size dependent adhesion strength and adhesion strength reinforcement by structural proteins, as observed experimentally [248] and studied what the effect was on cell shape. Previous models have explained cell responses based on how matrix stiffness influences cellular mechanisms. For instance, increased cell spreading on stiff matrices has been proposed to be regulated by a stiffness induced upregulation of cell traction forces [48], stress fiber stabilization [221] or motor protein recruitment [219]. In previous computational models, assumptions on cell dynamics were often motivated by adhesion dynamics and could explain stiffness sensing [46, 48, 249, 250] and durotaxis [225, 227, 228, 230].

Similarly, the mechanism for cell spreading proposed in our previous work [183], was based on focal adhesion dynamics. In this previous model, we suggested that protrusions are more likely to stick to highly strained matrices that have strain-stiffened. This was motivated by the observation that cells more efficiently build up forces on stiff matrices, which enables stabilization of focal adhesions [129]. In this work, we developed an explicit model for focal adhesion growth, to study how the mechanosensitive assembly of focal adhesions drives cell spreading and durotaxis. Previous computational models that included focal adhesions suggested that an intricate interplay between stress fiber remodeling and focal adhesion growth is required for cell spreading on compliant matrices [220, 221]. A model by Stolarska et al. [222] suggested that the mechanosensitive growth of focal adhesions alone could not explain increased cell spreading on stiff matrices [222]. In this model, rigid matrices induce increased cell contraction which resists cell spreading. We however suggest that the mechanosensitive growth of focal adhesions is sufficient to explain cell spreading as a function of substrate stiffness. In contrast to the model by Stolarska et al. [222], cells in our model are able to spread on rigid matrices, because the adhesion strength of large focal adhesions resist cell retractions on stiff matrices.

A previous coupled cell-based - focal adhesion model was used to study durotaxis [225]. In this model, the number of focal adhesions was assumed to be higher on stiff substrates and the distribution of focal adhesions was assumed to be more narrow on stiff substrates. Both the number and distribution of focal adhesion then controlled the deviation from the direction of motion: on stiff matrices cells move more persistent, causing it to durotact. Recently, it was also proposed that cells durotact by tugging on the matrix and changing their direction towards areas that the cell perceives as stiff [226]. Our model shows that the directed movement of cells emerges from the mechanosensitive growth of focal adhesions and that no inherent persistent or directed

cell migration is required.

A limitation of our model is that it cannot accurately predict increasing focal adhesion sizes as a function of substrate stiffness (see Figure 4.2D), while this has been observed experimentally [215]. This may be explained by modeling choices. In the CPM, cells only make retractions at the boundary of the cell, so in the middle of the cell, integrin clusters continue to grow even on soft matrices. Also, there is a constant pool of free integrin bonds, making the growth rate of new focal adhesions to go down due to existing focal adhesions. Furthermore, our lattice based model does not define spatial effects in integrin clustering. In reality, small clusters may merge into larger adhesions and the availability of integrins that can bind to ECM, active integrin, is spatially and temporally regulated. Cells produce integrins, that diffuse and are activated within the cell. This activation of integrin depends on interaction with other proteins, such as talin [251] and vinculin [252]. Furthermore, Stretching of p130cas induces its phosphorylation, which in turn activates the small GTPase Rap1 [253] which activates integrins [254]. So, to better reproduce focal adhesion growth in future models, we can include other relevant mechanisms such as diffusion and the activation of integrins [49, 221, 251, 255]. However, because we were interested in cell shape in this work, which can be predicted with our model, we find the level of detail of focal adhesion dynamics sufficient at the moment.

In summary, we propose that the mechanosensitive response of molecules in focal adhesions suffice to explain the response of cells to matrix stiffness. In agreement with experimental observations, cells spread more on stiff matrices and obtain an elongated shape if the matrix is stiff enough. Furthermore, cells durotact and move faster with steeper stiffness gradients. This model paves the way to study how specific molecular mechanisms within focal adhesions impact cell and tissue level responses to matrix mechanics. This can give rise to new targets of treatment and the design of tissue engineering experiments.

4.4 Methods

We developed a multiscale model where cell movement depends on force induced focal adhesion dynamics. The model couples a cell-based model, substrate model and focal adhesion model in the following way. The Cellular Potts Model (CPM) describes cell movement. The shape of the cell is used to describe the stall forces that the cell exerts on the focal adhesions attached to a flexible substrate. These forces affect the growth of the focal adhesions. We assume that focal adhesions are clusters of integrins that behave as catch-slip bonds. Its dynamics are described using ordinary differential equations (ODEs). Finally, we assume that the cell-matrix link is strengthened by matrix stresses, which we calculate using a finite element model (FEM). In all simulations described in this work, we employ the parameter values as described in Table 4.1.

4.4.1 Cellular Potts Model

To simulate cell movement, we used the Cellular Potts Model (CPM) [73]. The CPM describes cells on a lattice $\Lambda \subset \mathbb{Z}^2$ as a set of connected lattice sites. Since the simulations in this article are limited to one cell, we describe the CPM here for a single cell. To each lattice site $\vec{x} \in \Lambda$ a spin $s(\vec{x}) \in \{0, 1\}$ is assigned. This spin value indicates if the cell $s(\vec{x}) = 1$ or the extracellular matrix $s(\vec{x}) = 0$ occupies this site. So, the cell configuration is given by $C = \{\vec{x} : s(\vec{x}) = 1\}$. The cell configuration evolves by dynamic Monte Carlo simulation. During one Monte Carlo Step (MCS), copies of a spin $s(\vec{x})$ from a source site $\vec{x}$ into a neighboring target site $\vec{x}\prime$ are attempted. Such copies mimic active cellular protrusions and retractions. During a MCS, N copy attempts are made, with N the number of lattice sites in the grid. Whether a copy is accepted or not depends on a balance of forces, which are represented in a Hamiltonian H.

A copy is accepted if H decreases, or with a Boltzmann probability otherwise, to allow for stochasticity of cell movements:

$$P(\Delta H) = \begin{cases} 1 & \text{if } \Delta H + Y < 0 \\ e^{(-\Delta H + Y)/T} & \text{if } \Delta H + Y \geq 0. \end{cases} \tag{4.1}$$

Here $\Delta H = H_{\text{after}} - H_{\text{before}}$ is the change in H due to copying, and the cellular temperature $T \geq 0$ determines the extent of random cell motility. Furthermore, Y denotes a yield energy, an energy a cell needs to overcome to make a movement. Finally, to prevent cells from splitting up into disconnected patches, we use a connectivity constraint that rejects a copy if it would break apart a cell in two or more pieces.

We use the following Hamiltonian:

$$H = \underbrace{\lambda A^2}_{\text{compression}} + \underbrace{\sum_{\text{neighbours}(\vec{x},\vec{x}\prime)} J(s(\vec{x}), s(\vec{x}\prime))}_{\text{line tension}} - \underbrace{\lambda_C \frac{A}{A_h + A}}_{\text{cell-matrix adhesion}} \tag{4.2}$$

The first term of H denotes a area constraint or compression, where A is the area of cell and λ is the corresponding Lagrange multiplier. In the second term, $J(s(\vec{x}), s(\vec{x}\prime)$ are the adhesive energy between two sites $\vec{x}$ and $\vec{x}\prime$ with spins $s(\vec{x})$ and $s(\vec{x}\prime)$. When taking a sufficient large neighborhood, the second term describes a line tension, as it approximates the perimeter of a cell [256]. We take a neighborhood order of 10. The third term describes the formation of adhesive contacts of cells with the substrate, where the bond energies lower the total energy [192], causing the cells to spread. The parameter λ_C is the corresponding Lagrange multiplier. The energy gain of occupying more lattice sites saturates with the cell area, as the total number of binding sites is limited. The parameter A_h regulates this saturation.

To describe cell-matrix binding via focal adhesions, we implement the following yield energy in the CPM

$$Y = \lambda_N \frac{N(\vec{x}\prime) - N_0}{N_h + N(\vec{x}\prime)} \cdot \mathbf{1}_{s(\vec{x}\prime)=1} \cdot \mathbf{1}_{s(\vec{x})=0}, \tag{4.3}$$

where $N(\vec{x})$ is the size of the focal adhesion at the target site. This models that a retraction is energetically costly for a cell to make, because it needs to break the actin-integrin connection. We assume that the size of the actin-integrin link is proportional to the size of the focal adhesion, *i.e.* the number of integrin bonds [257], and that the strength of adhesion saturates [210] with a parameter N_h. The substraction of N_0 represents that an adhesion only creates extra linkage if it is greater than a nascent adhesions. Note that the Y can not become negative, because we assume that adhesions smaller than N_0, a nascent adhesion, breaks down due to its short lifetime, see section C. So, only adhesions larger than N_0 create a yield energy. In section C, we further adapt this yield energy to describe a matrix stress induced focal adhesion reinforcement.

4.4.2 Cell traction forces

Following Schwarz et al [97], we assume that traction forces are generated by myosin II molecular motors on the actin fibers, of which the velocity is given by

$$v(\vec{F}) = v_0\left(1 - \vec{F}/\vec{F}_s\right), \tag{4.4}$$

where v_0 is a free velocity. The traction forces are applied to the ECM, which we assume is in plane stress. The constitutive equation is given by $h\vec{\nabla}\underline{\underline{\sigma}} = \vec{F}$ where $\underline{\underline{\sigma}}$ is the ECM stress tensor and h is the thickness of the ECM. We assume that the ECM is isotropic, uniform, linearly elastic and we assume infinitesimal strain theory. We solve this equation using a Finite Element Model (FEM). In the FEM, traction field $\vec{f}$ and ECM deformation $\vec{u}$ are related by:

$$\mathbf{K}\vec{u} = \vec{f}, \tag{4.5}$$

where $\mathbf{K}$ is the stiffness matrix given by

$$\mathbf{K} = h\int \mathbf{B}^T \frac{E}{1-\nu^2}\begin{pmatrix} 1 & \nu & 0 \\ \nu & 1 & 0 \\ 0 & 0 & \frac{1-\nu}{2} \end{pmatrix}\mathbf{B}, \tag{4.6}$$

where $\mathbf{B}$ is the conventional strain-displacement matrix for a four-noded quadrilateral element [156] and E is the Young's modulus and ν is the Poisson's ratio of the ECM. For more details on this part of the model, we refer to our previous work [183, 258].

Following Schwarz *et al.* [97], the force build-up is given by the ODE:

$$\mathbf{K}\vec{v}(\vec{f}) = \frac{d\vec{f}}{dt}. \tag{4.7}$$

However, since this equation is complex and also expensive to solve, we, for now, ignore the interactions between neighbouring sites, *i.e.* we reduce $\mathbf{K}$ to it's diagonal components. This gives us:

$$\vec{F}(\vec{x},t) = \vec{F}_s(\vec{x}) + (\vec{F}_0(\vec{x}) - \vec{F}_s(\vec{x}))\exp(-t/t_k) \tag{4.8}$$

where $\vec{F}_0$ is the force already exerted by the actin, and t_k is given by $\frac{|\vec{F}_s|}{v_0 K}$ where K is given by the diagonal entry of **K** Since the cell configuration and therefore the traction forces change each MCS, the tension on the focal adhesions does not build up from zero, but from the tension that was built up during the previous MCS: $\vec{F}_0$ at the current MCS is given by $\vec{F}(t_{\mathrm{FA}})$ of the previous MCS.

To calculate $\vec{F}_s$, the stall force of the cells, we employ a first-moment-of-area (FMA) model, proposed and experimentally validated by Lemmon & Romer [132]. This model infers stall forces from the shape of the cell of the CPM, based on the assumption that a network of actin fibers in the cell acts as a single, cohesive unit.

$$\vec{F}_s(\vec{x}) = \frac{\mu}{A} \sum_{\text{line piece } \vec{x}\to\vec{y}\subset C} \vec{x} - \vec{y}, \tag{4.9}$$

We divided with the cell area A such that force increases roughly linear with cell area, as experimentally observed [128].

4.4.3 Focal adhesions

At each lattice site ($\vec{x}$) occupied by the cell ($s(\vec{x}) = 1$), a focal adhesion is modeled as a cluster of bound integrin bonds N. Each individual integrin bond behaves as a catch-slip bond, whose lifetime is maximal under a positive force [232]. Accordingly, the growth of a cluster of such bonds is described by an ODE derived by Novikova and Storm [232]:

$$\frac{dN(\vec{x},t)}{dt} = \gamma N_a(t)(1 - \frac{N(\vec{x},t)}{N_b}) - d(\phi(\vec{x},t))N(\vec{x},t) \tag{4.10}$$

with γ a binding rate, N_a the number of free bonds, and N_b the maximal number of bound bonds a lattice site can contain. This logistic growth term is a slight adaptation compared to Novikova and Storm [232]. The degradation of the focal adhesions $d(\phi)$ depends on the tension ϕ on the focal adhesion N. This degradation rate is given by

$$d(\phi(\vec{x},t)) = \exp\left(\frac{\phi(\vec{x},t)}{N(\vec{x},t)} - \phi_s\right) + \exp -\left(\frac{\phi(\vec{x},t)}{N(\vec{x},t)} - \phi_c\right) \tag{4.11}$$

where ϕ_s and ϕ_c describe the slip and catch bond regime in N/m^2, respectively. Here, $\phi(\vec{x},t) = \frac{|\vec{F}(\vec{x},t)|}{\Delta x^2}$ is the stress applied to the lattice site of the focal adhesion. We assume that the number of free bonds N_a is limited by the number of available integrin receptors in the entire cell, N_m. These N_m receptors can be recruited to each focal adhesion site and enable binding of a bond. Thus, $N_a(t) = N_m - \sum_{\{\vec{x}|s(\vec{x})=1\}} N(\vec{x},t)$. We let the focal adhesions grow after each MCS for t_{FA} seconds with time increments of Δt_{FA}. If $N(\vec{x}) = 0$ and $s(\vec{x}) = 1$, we set $N(\vec{x}) = N_0$, such that degraded focal adhesions have the potential to grow again. This models that the cell creates focal complexes, precursors of focal adhesions that contain a small amount of integrins and have a very short lifetime. During a MCS, a cell breaks adhesions if it retracts, so, we set $N(\vec{x}) = 0$ when a retraction occurs. We assume that if a cell extends, it binds a number of integrins to the

matrix. So, after an extension we set $N(\vec{x}) = N_0$. Furthermore, after the focal adhesions were allowed to grow, *i.e.* at $t = t_{\mathrm{FA}}$ we set all $N(\vec{x}) = 0$ if $N(\vec{x}) < N_0$. This models that the cell fails to build a focal adhesion from a focal complex/nascent adhesion, which subsequently breaks down quickly do to its short lifetime [259].

4.4.4 Substrate stresses

The forces that were build up during a MCS, $\vec{F}(t_{\mathrm{FA}})$, are plugged into a finite element model (FEM) to calculate the stress tensor $\underline{\underline{\sigma}}(\vec{x})$ on each lattice site. We assume that the integrin-cytoskeletal adhesion strengthens as a result of stress. We define

$$g(\underline{\underline{\sigma}}) = \begin{cases} \frac{1}{2}(\sigma_{xx} + \sigma_{yy}) & \text{if } \frac{1}{2}(\sigma_{xx} + \sigma_{yy}) \geq 0 \\ 0 & \text{if } \frac{1}{2}(\sigma_{xx} + \sigma_{yy}) < 0 \end{cases} \tag{4.12}$$

the positive hydrostatic stress of the stress tensor that describes how much stress the adhesion experiences. Now, we extend the yield energy as follows:

$$Y = \lambda_{\mathrm{N}} \frac{N(\vec{x}') - N_0}{N_h + N(\vec{x}')} \cdot \left(1 + p \frac{g(\underline{\underline{\sigma}}(\vec{x}'))}{\sigma_h + g(\underline{\underline{\sigma}}(\vec{x}'))}\right) \cdot \mathbf{1}_{s(\vec{x}')=1} \cdot \mathbf{1}_{s(\vec{x})=0} \tag{4.13}$$

We thus assume that stress strengthens the adhesion, with parameter p and that this strengthening saturates with parameter σ_h.

4.4.5 Stiffness gradient

To study durotaxis, we model a stiffness gradient in the x-direction on a lattice of 1250 μm by 500 μm. The Young's modulus of the substrate $E(Pa)$ is given by $E(x) = \max\{1, 6000 + (x - 250) \cdot \text{slope}\}$, with x in μm, such that the Young's modulus at the center of the cell at time $t = 0$ is 6000 Pa and is nonzero. The default value for the slope is 20 20 Pa/μm.

4.5 Supplementary methods

In the main text, we proposed that matrix stress induces adhesion strengthening but noted that matrix stress might also reinforce cell contractility. Supplementary Figure 4.12 shows the results of having $\vec{F}_s = \vec{F}_s \cdot \left(1 + p\frac{g(\underline{\underline{\sigma}}(\vec{x}'))}{\sigma_h + \bar{g}(\underline{\underline{\sigma}}(\vec{x}'))}\right)$ instead of equation 4.13 in the main text. Since matrix stresses are defined on the lattice sites while forces are defined on the nodes of the lattice, we needed to assume some interpolation. We choose to take

$$\vec{F}_s = \vec{F}_s \cdot \frac{1}{4} \sum_{\text{surrounding4nodes}} \left(1 + p\frac{g(\underline{\underline{\sigma}}(\vec{x}'))}{\sigma_h + \bar{g}(\underline{\underline{\sigma}}(\vec{x}'))}\right) \tag{4.14}$$

4.6 Supplementary tables

parameter	description	value	unit	value was
CPM				
Δx	lattice site width	2.5	μm	chosen
λ	area constraint	0.0002	N/m per lattice site^2	chosen
$J(0, \text{cell})$	adhesive energy	3000	Nm per lattice site	chosen
nbo	neighbourhood order	10	-	estimated based on accuracy of line tension [256]
λ_C	adhesion strength	600	Nm per lattice site	chosen
A_h	area saturation	1000	lattice sites	chosen
λ_N	focal adhesion strength	4	Nm	chosen
p	actin-integrin strength	1	-	chosen
σ_h	saturation actin-integrin binding	5000	N/m^2	chosen
T	cellular temperature	2	Nm	chosen
Forces				
μ	traction magnitude	0.001	Nm per lattice site	estimated based on endothelial traction stresses [199]
v_0	free velocity of myosin molecules	100	nm/s	estimated based on non-muscle myosin IIB [241, 243]
E	Young's modulus	10000	N/m^2	varies
ν	Poisson's ratio	0.45	-	chosen
τ	substrate thickness	10	μm	[159]
FAs				
γ	growth rate	0.05	/s	estimated [232]
N_0	size initial adhesion	5000	-	estimated based on nascent adhesions [259]
N_m	maximum free bonds	8000000	-	chosen

N_b	maximum size focal adhesion	39062	-	estimated based on number of integrins that fit in one lattice site [259]
ϕ_s	slip tension	4.02	pN/m^2	[232]
ϕ_c	catch tension	7.76	pN/m^2	[232]
t_{FA}	focal adhesion growth time	10	s	estimated based on protrusion lifetimes [260]
Δt_{FA}	time steps	0.01	s	chosen

Table 4.1: Parameter setting.

λ/T	1	2	3
0.0015	7.5106 ± 0.7971	5.3998 ± 1.1767	5.1622 ± 0.7922
0.002	6.7372 ± 1.1609	4.2945 ± 0.9978	31785 ± 1.1845
0.0025	5.5544 ± 1.3991	4.0823 ± 1.4943	3.0196 ± 1.3468

Table 4.2: Durotaxis speed in μm/h as a function of λ and T. Values: mean ± standard deviation of 25 simulations.

4.7 Supplementary figures

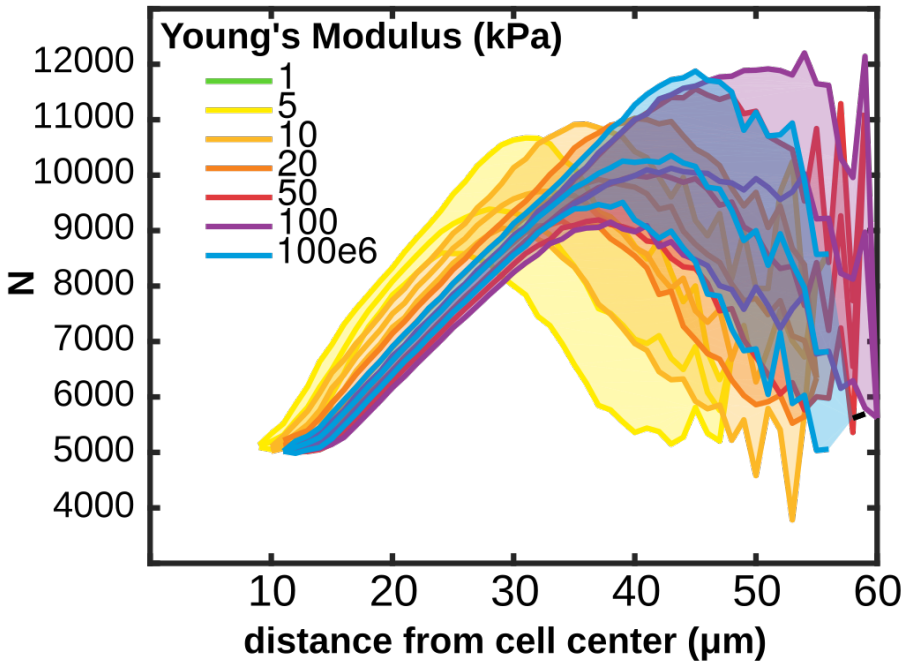

Figure 4.6: The number of integrin bonds per cluster (N) in model M1 as a function of distance from the cell center. All clusters at 2000 MCS from 25 simulations were pooled. Shaded regions show standard deviations.

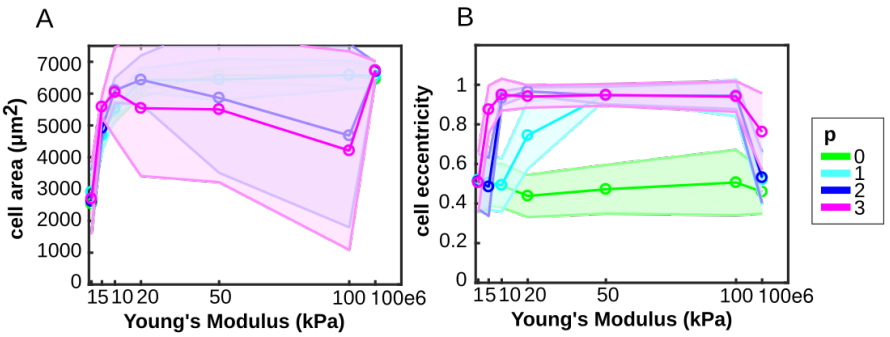

Figure 4.7: Model sensitivity to p. (A) Cell area as a function of substrate stiffness, shaded regions: standard deviations of 25 simulations; (B) Cell eccentricity as a function of substrate stiffness, shaded regions: standard deviations of 25 simulations.

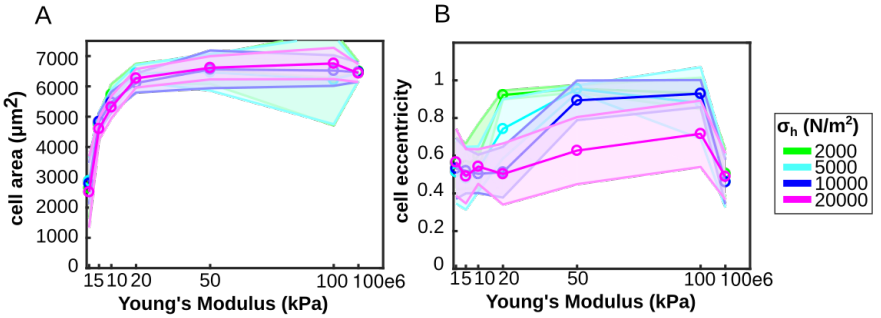

Figure 4.8: Model sensitivity to σ_h. (A) Cell area as a function of substrate stiffness, shaded regions: standard deviations of 25 simulations; (B) Cell eccentricity as a function of substrate stiffness, shaded regions: standard deviations of 25 simulations.

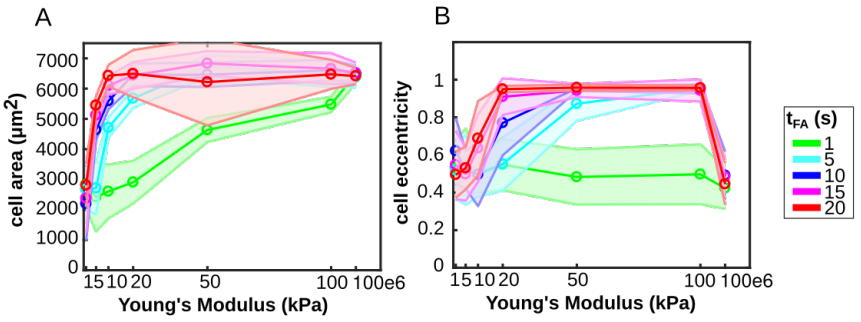

Figure 4.9: Model sensitivity to t_{FA}. (A) Cell area as a function of substrate stiffness, shaded regions: standard deviations of 25 simulations; (B) Cell eccentricity as a function of substrate stiffness, shaded regions: standard deviations of 25 simulations.

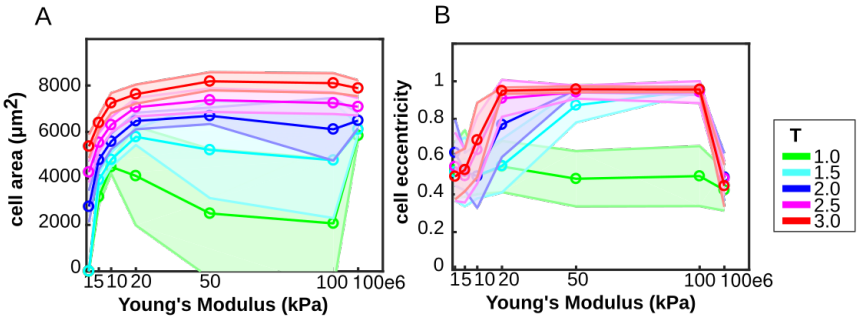

Figure 4.10: Model sensitivity to T. (A) Cell area as a function of substrate stiffness, shaded regions: standard deviations of 25 simulations; (B) Cell eccentricity as a function of substrate stiffness, shaded regions: standard deviations of 25 simulations.

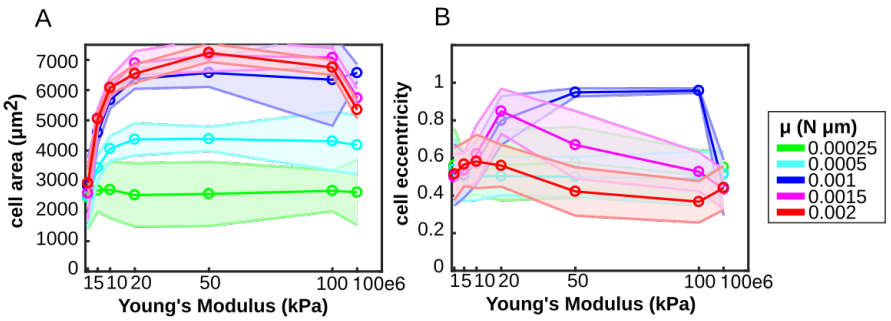

Figure 4.11: Model sensitivity to μ. (A) Cell area as a function of substrate stiffness, shaded regions: standard deviations of 25 simulations; (B) Cell eccentricity as a function of substrate stiffness, shaded regions: standard deviations of 25 simulations.

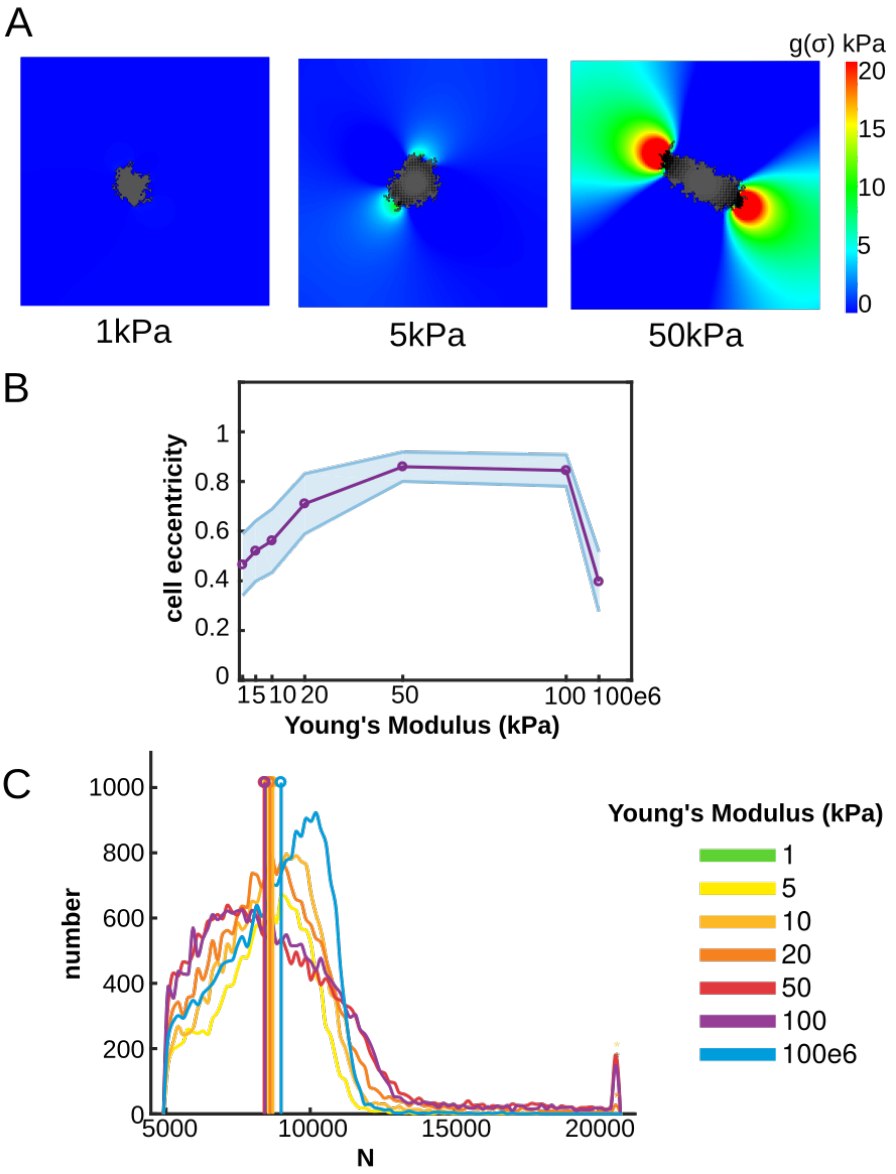

Figure 4.12: Cells elongate on substrates of intermediate stiffness if matrix stress reinforces traction force $\vec{F}_s$ with $p = 5$. (A) Example configurations of cells at 2000 MCS on substrates of 1,50 and 50 kPa. Colors: hydrostatic stress; (B) Cell eccentricity as a function of substrate stiffness, shaded regions: standard deviations of 25 simulations; (C) distribution of N, the number of integrin bonds per cluster, all adhesion at 2000 MCS from 25 simulations were pooled. We indicate the median. Color coding (C): See legend next to (C).